Src homology 2 domain containing protein 5 (SH2D5) binds the breakpoint cluster region protein, BCR, and regulates levels of Rac1-GTP*

Gray, E.J. and Petsalaki, E. and James, D.A. and Bagshaw, R.D. and Stacey, M.M. and Rocks, O. and Gingras, A.C. and Pawson, T.

Journal of Biological Chemistry
2014 SEP 19 ; 289(51): 35397-35408
Doi: 10.1074/jbc.M114.615112

American Society for Biochemistry and Molecular Biology

Signal Transduction:

Src Homology 2 Domain Containing Protein 5 (SH2D5) Binds the Breakpoint Cluster Region Protein, BCR, and Regulates Levels of Rac1-GTP

Elizabeth J. Gray, Evangelia Petsalaki, D. Andrew James, Richard D. Bagshaw, Melissa M. Stacey, Oliver Rocks, Anne-Claude Gingras and Tony Pawson

J. Biol. Chem. 2014, 289:35397-35408.
doi: 10.1074/jbc.M114.615112 originally published online October 20, 2014

THE JOURNAL OF BIOLOGICAL CHEMISTRY VOL. 289, NO. 51, pp. 35397–35408, December 19, 2014

Src Homology 2 Domain Containing Protein 5 (SH2D5) Binds the Breakpoint Cluster Region Protein, BCR, and Regulates Levels of Rac1-GTP*

Received for publication, September 30, 2014 Published, JBC Papers in Press, October 20, 2014, DOI 10.1074/jbc.M114.615112

Elizabeth J. Gray[‡§1], Evangelia Petsalaki[§], D. Andrew James[§¶], Richard D. Bagshaw[§2], Melissa M. Stacey[§], Oliver Rocks[§‖3], Anne-Claude Gingras[‡§4], and Tony Pawson[‡§†]

From the [‡]Department of Molecular Genetics, University of Toronto, Ontario M5S1A8, Canada, the [§]Lunenfeld-Tanenbaum Research Institute, Mount Sinai Hospital, Toronto, Ontario M5G1X5, Canada, [¶]Sanofi Pasteur, Toronto, Ontario M2R3T4, Canada, and the [‖]Max Delbrück Center for Molecular Medicine Berlin-Buch, Robert-Rössle-Strasse 10, 13125 Berlin, Germany

Background: Src homology 2 domain containing protein 5 (SH2D5) is a previously uncharacterized protein that resembles the Shc proteins in structural organization.
Results: SH2D5 binds to the breakpoint cluster region protein (BCR) in a phosphotyrosine-independent manner.
Conclusion: SH2D5 controls neuronal morphology via BCR and Rac1.
Significance: This is the first characterization of SH2D5 in neuronal signaling.

SH2D5 is a mammalian-specific, uncharacterized adaptor-like protein that contains an N-terminal phosphotyrosine-binding domain and a C-terminal Src homology 2 (SH2) domain. We show that SH2D5 is highly enriched in adult mouse brain, particularly in Purkinjie cells in the cerebellum and the *cornu ammonis* of the hippocampus. Despite harboring two potential phosphotyrosine (Tyr(P)) recognition domains, SH2D5 binds minimally to Tyr(P) ligands, consistent with the absence of a conserved Tyr(P)-binding arginine residue in the SH2 domain. Immunoprecipitation coupled to mass spectrometry (IP-MS) from cultured cells revealed a prominent association of SH2D5 with breakpoint cluster region protein, a RacGAP that is also highly expressed in brain. This interaction occurred between the phosphotyrosine-binding domain of SH2D5 and an N*xx*F motif located within the N-terminal region of the breakpoint cluster region. siRNA-mediated depletion of SH2D5 in a neuroblastoma cell line, B35, induced a cell rounding phenotype correlated with low levels of activated Rac1-GTP, suggesting that SH2D5 affects Rac1-GTP levels. Taken together, our data provide the first characterization of the SH2D5 signaling protein.

Intracellular signaling relies in part on a series of protein-protein interactions that are often mediated by the recognition of a modified residue such as a phosphotyrosine (Tyr(P)) through specialized interaction domains, including the Src homology 2 (SH2)[5] and Tyr(P)-binding (PTB) domains (1, 2). Proteins containing one of these domains often have additional interaction modules, which enable the proteins to serve as adaptors, facilitating the recruitment of additional signaling molecules to regulate intracellular signaling cascades (3). The SH2 domain-containing protein 5 (SH2D5) is an uncharacterized adaptor-like protein with an N-terminal PTB domain, and a C-terminal SH2-like domain (4). This domain architecture is shared with the Shc family of adaptor proteins (see Fig. 1, *A* and *B*). Despite this conserved domain organization, the SH2 domain of SH2D5 lacks the critical arginine (βB5) necessary for Tyr(P) binding. (It is replaced by a tryptophan (5).) SH2D5 also lacks the Y*x*N motifs that serve as Tyr(P)-docking sites for the SH2 domain of the Grb2 adaptor (see Fig. 1, *A* and *B*).

SH2D5 is a recently evolved, mammalian specific protein (4) that is highly enriched in brain at the transcript level (6) and has been detected in phosphoproteomic screens from murine brain lysates and postsynaptic density (PSD) fractions (7, 8). However, there are no functional studies elucidating the biological role or significance of this protein. Because of the shared domain architecture of SH2D5 with Tyr(P) recognition adaptor proteins, we reasoned that a first step in unraveling the function of SH2D5 would be to analyze its interaction profiles in unstimulated cells and cells in which tyrosine phosphorylation is induced by exposure to pervanadate. Here, we characterize a novel interaction of the SH2D5 PTB domain with breakpoint cluster region protein (BCR), a regulator of Rho GTPases (9, 10). We show enrichment of SH2D5 and BCR proteins in neuronal cell types. Finally, we report that SH2D5 depletion in neu-

* This work was supported by Canadian Institutes of Health Research Grants MOP-6849 and MOP-13466 (to T. P.) and Grant MOP-84314 (to A.-C. G.).
† This paper is dedicated to the memory of Dr. Tony Pawson, who died on August 7, 2013.
[1] A recipient of the Natural Sciences and Engineering Research Council of Canada graduate award and an Ontario Graduate Scholarship award. To whom correspondence may be addressed: Centre for Addiction and Mental Health Hospital, 33 Russell St., Rm. 4038, Toronto, ON M5S 2S1, Canada. E-mail: elizabeth.gray@camh.ca.
[2] A recipient of the Canadian Institute Health Research award.
[3] A recipient of the Human Frontier Science Program Long Term Fellowship.
[4] The Canada Research Chair in Functional Proteomics and the Lea Reichmann Chair in Cancer Proteomics. To whom correspondence may be addressed: Lunenfeld-Tanenbaum Research Institute at Mount Sinai Hospital, 600 University Ave., Rm. 992, Toronto, ON M5G 1X5, Canada. Tel.: 416-586-5027; Fax: 416-586-8869; E-mail: gingras@lunenfeld.ca.

[5] The abbreviations used are: SH2, Src homology 2; BCR, breakpoint cluster region; GAP, GTPase-activating protein; PAK, p21-activated kinase; GEF, guanine nucleotide exchange factor; FL, full length; GTPase, guanine triphosphate; PTB, phosphotyrosine binding; Tyr(P), phosphotyrosine; SH2D5, Src homology 2 domain containing protein 5; PSD, postsynaptic density; mSH2D5, mouse SH2D5; hSH2D5, human SH2D5; RBD, Rac binding domain.

ronal cells display low levels of Rac1-GTP and a cell-rounding phenotype.

EXPERIMENTAL PROCEDURES

Generation of SH2D5 Antibody—A polyclonal antibody was generated in two rabbits toward the 56 C-terminal amino acids of mouse (m)SH2D5, expressed as a GST fusion protein in a pGEX 4T-1 vector, and tested for immunoreactivity. Antiserum was affinity-purified using AminoLink Plus Immobilization Pierce affinity columns (Pierce catalog no. 44894) according to the manufacturer's instructions. Briefly, two columns were utilized for affinity purification. For the first column, 6 mg of GST protein were covalently coupled to the AminoLink resin, and a 1:1 dilution of antisera and PBS was loaded onto the column and incubated at 4 °C for 4 h. The second affinity column was prepared by coupling 4 mg of the GST-fused mSH2D5 immunogenic peptide. Flow-through from the first column was incubated at 4 °C for 3 h on the second column, and bound antibody was eluted with 10 × 1-ml fractions of 1% glycine, pH 1.5–2.0, followed by neutralization with Tris. Fractionated elutions were dialyzed overnight at 4 °C in 4 liters of PBS, and fractions were tested for yielding the highest titer for mSH2D5 as determined by immunoblot from lysates prepared by transient transfection of 3×FLAG-mSH2D5 into human embryonic kidney (HEK)293T cells. High titer fractions for mSH2D5 were pooled, and protein concentration was determined using the BCA assay. Aliquots of purified antibody were stored at −80 °C until further use.

Plasmids—Full-length mSH2D5 (NCBI accession no. BC036961) and human (h) SH2D5 (synthesized by Genscript, NCBI RefSeq no. NP_001096631.1) cDNAs were cloned into a Creator parent donor vector (Clontech), pDNA MCS SA or pDNA MCS SA LacZ α using the restriction sites AscI and PacI. Utilizing the Cre-recombinase reaction (11), full length h- or mSH2D5 were excised into donor vectors containing an N-terminal 3×FLAG tag, N-terminal 2×Myc tag, N-terminal mCherry, or citrine (11). The W321R mutation within the hSH2D5 SH2 domain was prepared by site-directed mutagenesis using the Stratagene QuikChange kit (no. 200522-5) and sequence-verified. Deletion mutants of mSH2D5 were prepared by PCR amplification of various regions of full length protein, whereas the PTB and SH2 domain boundaries were defined by the SMART database (12). PCR fragments were cloned into creator donor vectors and spliced into N-terminal 3×FLAG tag or N-terminal 2×Myc tag acceptor vectors. Mutations within BCR were prepared by site-directed mutagenesis using the Stratagene QuikChange kit (no. 200522-5): N179A/F182A/N252A/F255A within the N-terminal region. All mutations were sequence-verified.

Cell Culture, Transfection, and Stimulation—HEK293T cells, DLD-1, K562, KBM-3, Neuro2A, and B35 were cultured in Dulbecco's modified Eagle's medium or modified Eagle's medium supplemented with 10% fetal bovine serum (HyClone). Cells were transiently transfected using polyethyleneimine, Lipofectamine 2000 (Invitrogen), or RNAi Max (Invitrogen) and when required treated with 0.1 mM pervanadate for 40 min. Pervanadate was prepared by combining sodium orthovanadate and hydrogen peroxide for 10 min on ice, prior to applying to intact cells. Activity of pervanadate was verified by probing lysates for phosphotyrosine by immunoblot.

Lysate Preparation and Immunoblotting—Lysates were prepared from wild-type male C57BL/6 mice tissues, age 4–6 weeks, HEK293T or Neuro2A cells. Murine tissues and cell pellets were lysed in 50 mM HEPES, pH 7.5, 150 mM NaCl, 10% glycerol, 1% Triton X-100, 15 mM MgCl, supplemented with 10 μg/ml aprotinin, 10 μg/ml leupeptin, 1 mM sodium vanadate, 1 mM PMSF and 1 mM DTT. Murine brain samples were lysed in a glass homogenizer, and protein concentration was determined by the BCA assay, and concentrations were normalized accordingly. Whole brain lysates for endogenous immunoprecipitations were prepared by solubilizing murine whole brains in 1% Triton X-100, 50 mM HEPES, pH 7.5, 150 mM NaCl, freshly supplemented with protease inhibitors 10 μg/ml aprotinin, 10 μg/ml leupeptin, 1 mM sodium vanadate, 1 mM phenylmethylsulfonyl fluoride, and 1 mM dithiothreitol.

PSDs were prepared from male C57BL/6 mice, age 6–8 weeks, using a procedure modified from Dunah *et al.* (13). Briefly, whole brains were resuspended in 0.32 M sucrose, 4 mM HEPES pH 7.4, supplemented with protease and phosphatase inhibitors (10 μg/ml aprotinin, 10 μg/ml leupeptin, 1 mM pervanadate, 1 mM phenylmethylsulfonyl fluoride, hereafter referred to as buffer 1). Homogenate was centrifuged at 4 °C for 10 min at 10,000 × *g* (Allegra 12F Beckman Coulter), and the pellet, P1 (nuclei, cellular debris) was saved. The supernatant (S1) was centrifuged again for 15 min at 4 °C at 12,000 × *g* (Beckman Ultracentrifuge, MLA-80), and the supernatant from this spin was denoted S2 (synaptosome depleted fraction). The pellet P2 (crude synaptosomal fraction) was rinsed in 50 mM HEPES, pH 7.4, 2 mM EDTA, supplemented with protease and phosphatase inhibitors, hereafter referred to as buffer 2. The P2 fraction was then resuspended again in buffer 2. The slurry was centrifuged for 20 min at 4 °C at 32,000 × *g* (Beckman Ultracentrifuge, MLA-80), and the supernatant LS1 (synaptosomal cytosolic fraction) was collected. The pellet LP1 (mitochondria, pre- and postsynaptic membranes) was washed with buffer 2 and resuspended again in buffer 2. Fractions S2 and LS1 were centrifuged again for 2 h at 4 °C at 165,000 × *g* (Beckman Ultracentrifuge, MLA-80). Supernatants were then collected and termed S3 (cytosol) and LS2 (synaptosol).

Pellets from this spin were resuspended in buffer 2 and sonicated using a Probe Sonicator (Vibra Cell Sonics Material, Inc.) at an amplitude of 50 at 4 °C for 5–10-s pulses, and slurries were denoted P3 (microsomes) and LP2 (crude synaptic vesicle fraction), respectively. LP1 was then washed in buffer 2, resuspended again in buffer 2 and sonicated for 5–10 s. Triton X-100 was then added to a final concentration of 1% to LP2 samples that were incubated on ice for 1 h. Solutions were then spun for 20 min at 4 °C at 32,000 × *g* (Beckman Ultracentrifuge, MLA-80), and the supernatant PSD S1 (Triton extracted postsynaptic density supernatant 1) was collected. The pellet PSDI (Triton extracted insoluble postsynaptic density fraction) was resuspended in buffer 2, and sodium lauroyl sarcosinate and sarcosyl were added to a final concentration of 3% each. Samples were centrifuged for 1 h at 4 °C at 200,000 × *g* (Beckman Ultracentrifuge, MLA-130), and the supernatant was collected, termed PSDII (Triton and sarcosyl postsynaptic density fraction).

Antibodies used for immunoblotting or immunoprecipitation were obtained from the following commercial sources: mouse monoclonal anti-Tyr(P) 4G10 (Millipore catalog no. 05-321), mouse monoclonal anti-FLAG M2 (Sigma catalog no. 3165), rabbit polyclonal anti-BCR N-20 (Santa Cruz catalog no. 885 and Cell Signaling Technology catalog no. 3901), mouse monoclonal anti-PSD 95 (Abcam catalog no. 7ES-1B8), mouse monoclonal anti-tubulin DM1A (Sigma catalog no. 9026), mouse monoclonal c-Myc 9E10 (Santa Cruz Biotechnology catalog no. 40), rabbit polyclonal anti-GFP (Abcam catalog no. 290), mouse monoclonal anti-Rac1 23A8 (Millipore catalog no. 05-389), and mouse monoclonal GAPDH (Cell Signaling Technologies catalog no. ^{14}C10).

Immunohistochemistry of Brain Sections—Whole brains from wild-type male C57BL/6 mice, age 6–8 weeks, were fixed in 4% paraformaldehyde PFA and mounted in paraffin sections. SH2D5 antigen retrieval was conducted by incubating slides for 20 min in 10 mM sodium citrate buffer, followed by a PBS wash for 5 min. Blocking was carried out with Dako protein block, serum-free, for 30 min (Dako, catalog no. X0909). Purified anti-SH2D5 was used at a 1:50 dilution and incubated overnight at 4 °C, followed by three PBS washes for 5-min each. Slides were incubated in secondary antibody, biotinylated goat anti-rabbit IgG (1:200, Vector Laboratories, BA-1000), for 30 min at room temperature followed by three washes in PBS for 5-min each. Slides were then counterstained with hematoxylin (1.0 g/liter) for 30 s.

Deparaffinization for BCR immunohistochemistry IHC was carried out using xylene I, II, and III for 5-min each. Slides were rehydrated in 100% ethanol and double-distilled water for 5 min. Antigen retrieval was conducted using proteinase K (10 μg/ml) for 30 min at room temperature, followed by three washes in PBS. Blocking was carried out with a Dako protein block (Dako, catalog no. X0909). Primary anti-BCR antibody (Cell Signaling Technology, catalog no. 3901) was incubated in a 1/50 dilution at 4 °C overnight followed by three washes in PBS for 5-min each.

Immunoprecipitation and Mass Spectrometry Analysis—Immunoprecipitations were carried out using 2 μg of anti-FLAG mouse monoclonal antibody (Sigma catalog no. 3165) with 10 μl of packed protein G beads, 2 μg of anti-GFP rabbit polyclonal (Abcam catalog no. 290) with 10 μl of packed protein A-Sepharose beads, or 2 μg of anti-c-Myc mouse monoclonal (Santa Cruz Biotechnology, catalog no. 40) with 10 μl of packed protein A-Sepharose. For all immunoprecipitations, the antibody and the beads were added simultaneously to the cell lysates. Immunoprecipitations were carried out for 2 h at 4 °C on a Gyro Mini nutating mixer (LabNet S0500). Unbound proteins were removed by three washes in lysis buffer for 10 min each at 4 °C. For immunoblot analysis, proteins were eluted by boiling beads in 2× SDS sample buffer for 10 min. For mass spectrometry analysis, bait and prey proteins were eluted from the beads using 90 μl of 0.2% phosphoric acid and digested on a strong cation exchange column.

All mass spectrometry experiments were performed on a QSTAR Elite QqTOF mass spectrometer equipped with a nanospray III ion source (AB Sciex Concord, ON, Canada), coupled to an Eksigent 1D+ Nano LC (Dublin, CA). Samples were injected directly onto in-house "packed tip" columns. A 4-μm tip was pulled at the end of a 25-cm piece of 360 μm, inner diameter × 75 μm fused silica tubing using a Model 2000 Micropipette Laser Puller (Sutton Instrument Co.). A methanol slurry of 3 μm of ReprosilGold 120 C-18 stationary phase medium was prepared in a 1.5-ml glass vial and placed into a pressure bomb. 120 mm of stationary phase was packed into the 360 μm, inner diameter × 75 μm fused silica pulled-tip using the pressure vessel set at 1500 psi. Samples (at an injected volume of 7 μl) were run using a 90-min gradient from 5–30% solvent B (solvent A, water with 0.1% formic acid; solvent B, acetonitrile with 0.1% formic acid) at a flow rate of 250 nl/min. Samples were injected into the mass spectrometer in the following order: control sample, followed by bait protein sample. Standard BSA injections were run between samples to limit cross-contamination.

For database searches, acquired RAW files were converted to mascot generic format (mgf) files using the ProteoWizard (14) tool with default parameters and were searched with Mascot (Matrix Sciences, London, UK, version 2.3) against the RefSeq database (version 42 for human (total entries searched, 39,125) and version 41 for mouse (total entries searched, 36,378)). Searches were performed on the mgf files with carbamidomethyl (C) set as a fixed modification and deamidation (NQ), oxidation (M), phosphorylation (S/T), and phosphorylation (Y) set as variable modifications. Trypsin was selected for enzyme digestion with up to two missed cleavages. Pulsar type fragmentation was selected with peptide mass tolerance set to 100 ppm and fragment mass tolerance set to 0.15 Da. As a negative control, FLAG-GFP immunoprecipitations were performed in both HEK293T and Neuro2A in a manner similar to the SH2D5 pulldowns to detect background contaminants. The results from Mascot were then run through the Trans Proteomics Pipeline (15) using the ProHits interface (16).

Identified proteins were filtered as follows: first, the proteins that were found in negative control pulldowns were removed. We then removed known contaminants in similar FLAG purifications (17) as well as antibody, keratin, and albumin proteins. Proteins with a Trans Proteomics Pipeline ProteinProphet score >0.95 and with at least eight peptides identified in at least one experiment were kept in our data sets. For generating the list of interactors, we mapped the mouse proteins identified onto their human orthologs using the MGI database. To further reduce the probability of including frequent flyer proteins in our final list, we used an additional strict filtering technique. In this method, background proteins identified in >15% of samples analyzed in the Pawson laboratory (~550 samples)[6] were removed from the data set. Lastly, only proteins detected across both the Neuro2A and the HEK293T cell lines were kept; this resulted in only two proteins, the SH2D5 bait, as expected, and the breakpoint cluster region protein BCR.

RNA Interference of SH2D5—SH2D5 levels were depleted in the rat neuroblastoma cell line B35 using Dharmacon SMART Pool ON-TARGETplus reagents (Dharmacon, Thermo Scientific, Lafayette, CO). Cells were seeded in a 24-well plate at a

[6] E. J. Gray, E. Petsalaki, D. A. James, R. D. Bagshaw, M. M. Stacey, O. Rock, A.-C. Gingras, and T. Pawson, unpublished data.

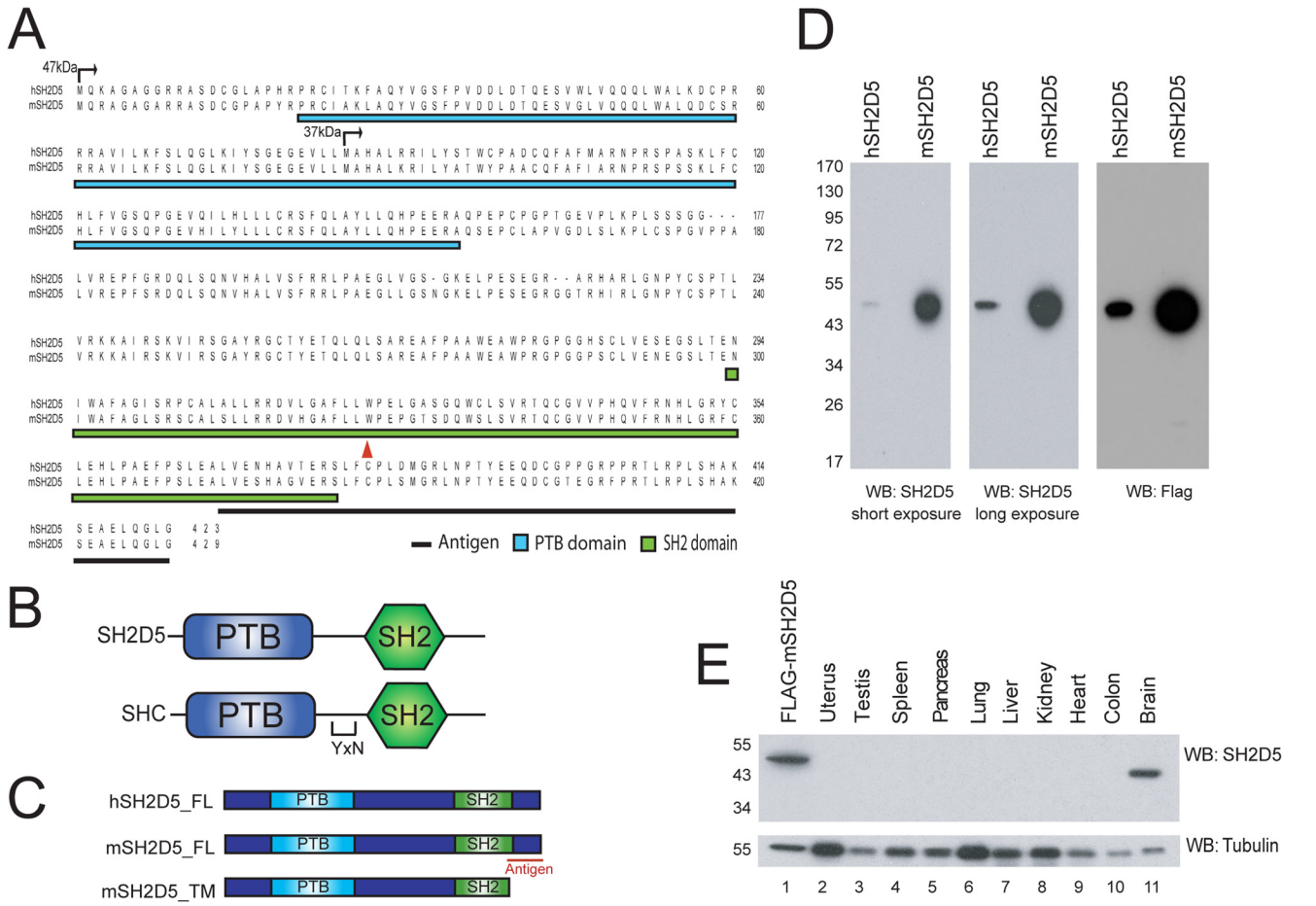

FIGURE 1. **Domain architecture of the SH2D5 protein and expression pattern.** *A*, two isoforms of SH2D5 are predicted (*black arrows*). The longer SH2D5 isoform contains an N-terminal PTB (*blue underline*) and C-terminal SH2 domain (*green underline*). The SH2 domain lacks the critical arginine necessary for phosphotyrosine binding (*red arrow*). A 56-amino acid antigen (*black underline*) was used to generate a rabbit polyclonal antibody toward SH2D5. *B*, SH2D5 shares a similar domain architecture to the Shc adaptor. *C*, constructs utilized for characterizing the SH2D5 antibody. A deletion mutant of mSH2D5 (*TM*), which is missing the antigenic region (*red underline*) was used as a negative control. *D*, the SH2D5 antibody recognizes overexpressed recombinant h- and mSH2D5 in immunoblot. *E*, SH2D5 expression in tissue lysates from C57B/6 WT mice aged 4–6 weeks. The FLAG tag results in a 3-kDa mass shift for recombinant mSH2D5 compared with endogenous mSH2D5, which migrates at 47 kDa. *WB*, Western blot.

density of 1.7×10^5 cells/well in antibiotic-free medium and at the time of seeding were transfected with 50 nM of siRNA using Lipofectamine RNAi Max according to manufacturers protocol. GAPDH, scrambled siRNA, and the deconvoluted siRNAs from the SH2D5 SMARTPool were transfected at a 50 nM concentration.

GST-PAK-RBD Pulldown Assays—Levels of activated Rac1 were measured by utilizing a standard glutathione *S*-transferase p21-activated kinase-Rac binding domain (GST-PAK-RBD) binding assay, which selects for activated levels of endogenous Rac1. B35 neurons were seeded at a density of 8×10^6 cells/15-cm plates and at the time of seeding, cells were depleted of SH2D5 using siRNA as above. Cells were lysed in 1 ml of RBD lysis buffer: 1% Nonidet P-40, 10% glycerol, 50 mM Tris-HCl (pH 7.5), 15 mM $MgCl_2$, 150 mM NaCl, freshly supplemented with 1 mM DTT, 10 μg/ml of aprotinin, 10 μg/ml of leupeptin, 100 mM sodium vanadate, and 100 mM PMSF. Lysates (quantified by the BSA assay) were incubated for 45 min with 120 μl of GST-PAK-RBD corresponding to 25 μg of protein. Beads were pelleted by centrifugation at 3000 rpm for 5 min, the supernatant discarded, and beads were washed three times with RBD buffer for 5 min each. Beads were then boiled in 70 μl of 2× SDS sample buffer, and proteins resolved on an SDS-PAGE gel were transferred to a PVDF membrane for immunoblot detection using specific antibodies.

RESULTS

SH2D5 Expression in Brain—To monitor SH2D5 expression, we generated a rabbit polyclonal antibody toward the last C-terminal 56 amino acids of mSH2D5 (Fig. 1, *A* and *C*). In an immunoblot, the SH2D5 antibody readily recognized overexpressed recombinant human (h) and mSH2D5 from a total cell lysate of HEK293T cells (Fig. 1*D*). We then examined endogenous SH2D5 protein expression in murine tissues. SH2D5 has a predicted molecular mass of 47 kDa, and a possible second isoform is predicted at 37 kDa because of an alternative initiator methionine (this form should also be recognized by our antibody). We find a single 47-kDa SH2D5 isoform that is highly expressed in brain (Fig. 1*E*).

SH2D5 Binds Minimally to Tyr(P) Proteins but Interacts with BCR—Given the unusual nature of the SH2D5 SH2 domain (Fig. 1*A*), we assessed whether SH2D5 could bind proteins in a phosphotyrosine-dependent manner. HEK293T cells were transiently transfected with 3×FLAG-tagged mSH2D5, and

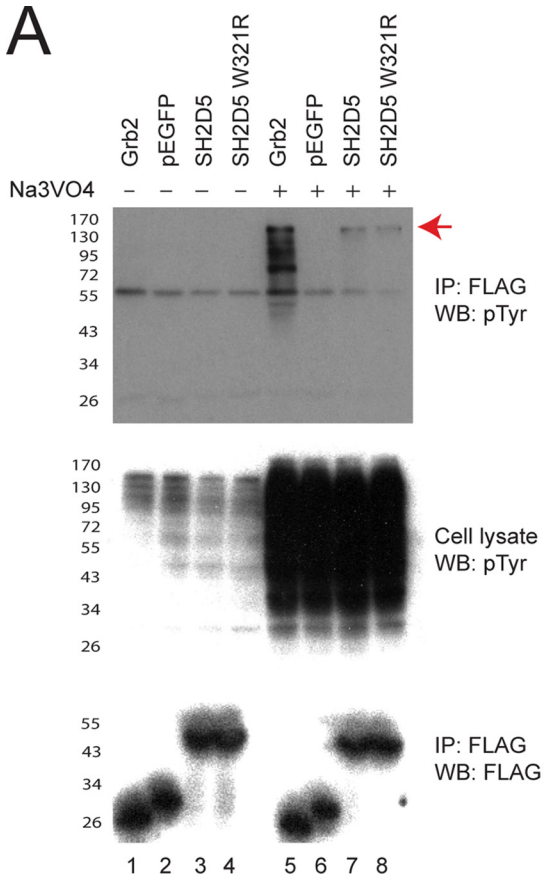

B

Sample	Accession	Gene	Spectral counts	Unique peptides	Coverage (%)
293T pervanadate	P11274	BCR	166	93	64.4
293T pervanadate	Q6ZV89	SH2D5 (bait)	122	22	44.5
293T untreated	P11274	BCR	31	24	19.6
293T untreated	Q6ZV89	SH2D5 (bait)	409	20	32.7
Neuro2A pervanadate	Q6PAJ1	BCR	182	106	63.7
Neuro2A pervanadate	Q8JZW5	SH2D5 (bait)	61	33	66.4
Neuro2A untreated	Q6PAJ1	BCR	226	116	63.1
Neuro2A untreated	Q8JZW5	SH2D5 (bait)	73	27	69

FIGURE 2. **Characterization of the binding properties of SH2D5.** *A*, as SH2D5 lacks the critical βB5 arginine necessary for Tyr(P) ligand recognition, mutagenesis was used to reintroduce the arginine residue W321R. HEK293T cells were transiently transfected with 3×FLAG-tagged Grb2 (*lanes 1* and *5*), FLAG-tagged green fluorescent protein (*GFP*) (*lanes 2* and *6*), 3×FLAG-tagged hSH2D5 (*lanes 3* and *7*), or 3×FLAG-tagged W312R SH2D5 (*lanes 4* and *8*). Intact cells were left untreated (*lanes 1–4*) or treated with 0.1 mM pervanadate for 40 min (*lanes 5–8*). Proteins were immunoprecipitated with FLAG antibodies, and lysates were probed with an anti-Tyr(P) (*pTyr*) antibody (*middle panel*). A tyrosine-phosphorylated protein resolving at ~160 kDa, is present in the wild-type and W321R SH2D5 immunoprecipitate (*red arrow*). *B*, results of the immunopurification coupled to mass spectrometry experiments. Human HEK293T cells or mouse Neuro2A cells were transiently transfected with 3×FLAG-tagged hSH2D5 and treated (or not) with pervanadate as described above. FLAG IP-MS was performed as detailed under "Experimental Procedures." BCR and the SH2D5 bait were the only two proteins detected across the two different cell lines. Their spectral counts, unique number of peptides (as searched in the human or mouse library, respectively), and sequence coverage (in percentage) are listed. *WB*, Western blot.

intact cells were treated or not treated with 0.1 mM pervanadate for 40 min to increase cellular Tyr(P) levels (Fig. 2*A*). SH2D5 was immunoprecipitated with anti-FLAG antibodies, and lysates were immunoblotted with an anti-Tyr(P) antibody. SH2D5 bound minimally to Tyr(P) proteins compared with the Grb2 adaptor, which binds multiple Tyr(P)-containing proteins through its SH2 domain. The only Tyr(P) protein associating with SH2D5 migrated at 160 kDa (Fig. 2*A*) (see "Discussion"). We attempted to restore SH2 domain Tyr(P) binding by mutating the tryptophan found at the βB5 position (residue 321) to arginine, but mutagenesis of this residue did not increase the ability of SH2D5 to enrich tyrosine phosphorylated proteins, suggesting that its SH2 domain may have additional defects in Tyr(P) recognition (Fig. 2*A*).

We used immunoprecipitation coupled to mass spectrometry (IP-MS) to identify binding partners for SH2D5. HEK293T and Neuro2A cells were transiently transfected with 3×FLAG-mSH2D5, and cells were treated or not with pervanadate. SH2D5 was immunoprecipitated with anti-FLAG antibodies, and precipitated proteins were identified using liquid chromatography coupled to mass spectrometry. Consistently, across all cell lines and regardless of Tyr(P) levels, BCR was identified as the strongest interaction partner of SH2D5 (Fig. 2*B* and Table 1; see "Experimental Procedures").

SH2D5 Binding to BCR Is Not Tyr(P)-dependent—BCR is a multidomain protein with an N-terminal region, also referred to as a pseudokinase domain, followed by RhoGEF, pleckstrin homology, C2, and RhoGAP domains. Although BCR contains both a GEF and a GAP domain, the activity of the GEF domain is ambiguous (18, 19). BCR is 68% homologous to ABR (active BCR-related), but ABR lacks the N-terminal region present in BCR (Fig. 3*A*) (20). To address whether the SH2D5 and BCR interaction is Tyr(P)-dependent, HEK293T cells were transfected with 3×FLAG-mSH2D5, and cells were treated with pervanadate or left untreated. Lysates were immunoprecipitated with anti-FLAG antibodies to enrich for SH2D5, and immunoprecipitates were probed for endogenous BCR. SH2D5 bound endogenous BCR regardless of Tyr(P) levels, suggesting a Tyr(P)-independent interaction (Fig. 3*B*). We then probed for the SH2D5-BCR interaction in mouse brain by immunoprecipitating endogenous SH2D5 or BCR from mouse brain lysates. Indeed, BCR was detected in the endogenous SH2D5

TABLE 1

mSH2D5 interaction partners assembled from overexpressing 3×FLAG-tagged mSH2D5 in either human embryonic kidney (293T) cells treated with or without 0.1 mM pervanadate for 40 min

mSH2D5 was immunoprecipitated with FLAG antibodies, and interactors were identified via liquid chromatography/mass spectrometry. Interactors are listed with common names (interactor ID), unique peptide counts, sequence coverage (%), and the TransProteomics Pipeline (TPP) score. Data are significant at TPP score, >0.95, and were generated using an additional filtering step (refer to "Experimental Procedures" section). Proteins that were identified in the mouse cell line Neuro2A were mapped onto their human orthologs.

					0.1mM Pervanadate		
		HEK293T			HEK293T		
Interactor	Full name	Unique peptide counts	Coverage (%)	TPPscore	Unique peptide counts	Coverage (%)	TPPscore
BCR	breakpoint cluster region protein	24	19.6	1.0	93	64.4	1.0
SH2D5-bait	SH2 domain containing protein 5	20	32.7	1.0	22	44.5	1.0
ANAPC7	anaphase promoting complex subunit 7	11	19.7	1.0			
ANAPC4	anaphase promoting complex subunit 4	9	13.0	1.0			
CDC16	cell division cycle 16 homolog	9	12.7	1.0			
DNAJC7	DnaJ (Hsp40) homolog, subfamily C, member 7				10	18	1.0
GAPVD1	GTPase activating protein and VPS9 domains 1	28	19.2	1.0	17	15.4	1.0
GLDC	glycine dehydrogenase	6	7.2	1.0	12	14.4	1.0
PPP6R3	protein phosphatase 6, regulatory subunit 3	9	13.3	1.0	6	9.8	1.0
DICER1	dicer 1, ribonuclease type III	10	6.3	1.0	3	2.6	1.0

					0.1mM Pervanadate		
		Neuro2A			Neuro2A		
Interactors		Unique peptide counts	Coverage (%)	TPPscore	Unique peptide counts	Coverage (%)	TPPscore
BCR	breakpoint cluster region protein	116	63.1	1.0	106	63.7	1.0
SH2D5-bait	SH2 domain containing protein 5	27	69	1.0	33	66.4	1.0
TUBA1A	tubulin, alpha 1a	11	30.6	1.0	12	37.5	1.0
ABR	active BCR-related protein	30	45.3	1.0	26	35.5	1.0

immunoprecipitates, and SH2D5 could be detected in the endogenous BCR immunoprecipitates. Neither BCR nor SH2D5 were detected in the rabbit IgG negative control (Fig. 3*C*). To ensure that the anti-SH2D5 antibody was not binding directly to BCR, we performed immunoprecipitations against recombinant FLAG-tagged full-length SH2D5 and the FLAG-tagged truncated SH2D5 mutant, which lacks the region to which the antibody was raised. We then probed the immunoblots for BCR. BCR is only detected in the full-length SH2D5 immunoprecipitate, and not with the truncated mutant, supporting the notion that the anti-SH2D5 antibody does not cross-react with BCR (Fig. 3*D*).

The PTB Domain of SH2D5 Interacts with a Specific NxxF Motif within the N-terminal Region of BCR—We mapped the region of SH2D5 necessary for binding BCR using a series of 3×FLAG-tagged deletion mutants of mSH2D5 (Fig. 4*A*). These experiments showed that the PTB domain of SH2D5 is both necessary and sufficient to bind full-length endogenous BCR (Fig. 4*B*). Similarly, we made deletion mutants of BCR to address which region is recognized by the SH2D5 PTB domain (Fig. 4*C*) and found that the N-terminal region of BCR was sufficient to bind both full-length SH2D5 and its isolated PTB domain (Fig. 4*D*). PTB domains commonly recognize motifs containing a core NP*x*Y sequence, but whereas some PTB domains only efficiently recognize such sites once they are phosphorylated, not all PTB domains require Tyr(P) for binding (21). For example, the Numb PTB domain binds N*xx*F motifs (22). The N-terminal region of BCR lacks NP*x*Y sites, but contains two N*xx*F sequences in this region, NVEF and NPRF, respectively. To test whether these NxxF motifs in BCR may serve as ligands for the SH2D5 PTB domain, we mutated their asparagine and phenylalanine residues to alanines and tested for the ability of variants containing individual or double N*xx*F site mutations to bind SH2D5 (Fig. 4*E*). The resulting data showed that the more C-terminal N*xx*F motif in the N-terminal region of BCR is necessary for binding to the SH2D5 PTB domain and to the full-length protein, whereas the N-terminal motif appears to be dispensable (Fig. 4, *E*–*G*).

SH2D5 and BCR Expression—As BCR is expressed in brain and is enriched in the PSD (9), we compared SH2D5 expression with that of BCR. Both proteins were found throughout different brain regions though their expression pattern did not fully overlap (Fig. 5*A*). Interestingly, SH2D5 expression increases through development and reaches a maximum in adult brain. We found that BCR expression decreases through development (Fig. 5, *B* and *C*), which is supported by Oh *et al.* (9), who observed decreased levels of BCR expression as mice age. It is tempting to speculate that this differential expression may be due to mutual regulation, although this remains to be investigated. We also found that both SH2D5 and BCR share partial enrichment in the PSD (Fig. 5*D*). There again, however, the overlap is only partial: SH2D5 is readily extracted in the PSD soluble fraction with Triton X-100 and shows enrichment in the pellet (PSD1). Although BCR is also found in the same frac-

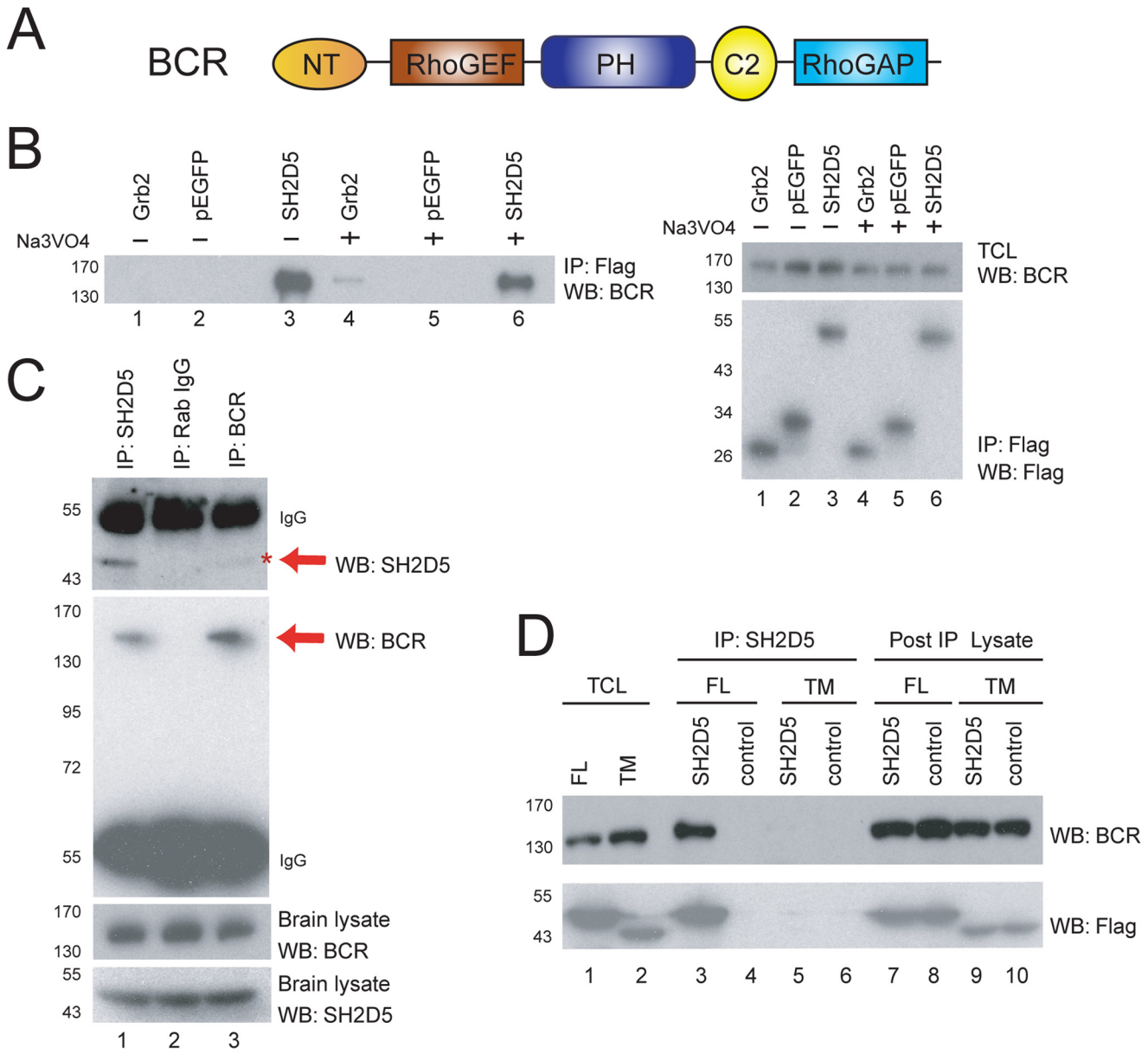

FIGURE 3. **Validation of the SH2D5-BCR interaction.** *A*, BCR contains an N-terminal region (*NT*) and GEF, PH, C2, and GAP domains. *B*, HEK293T cells were transiently transfected as indicated with 3×FLAG-tagged Grb2 (*lanes 1* and *4*), 3×FLAG-tagged pEGFP (*lanes 2* and *5*) or with 3×FLAG-tagged SH2D5 (*lanes 3* and *6*). Intact cells were treated with (*lanes 4–6*) or without (*lanes 1–3*) 0.1 mM pervanadate for 40 min. Proteins were immunoprecipitated with FLAG antibodies, and lysates were probed for endogenous BCR (*left*). Endogenous BCR was expressed at similar levels (*right*; *top*) and recombinant proteins were precipitated in similar levels (*right*; *bottom*). *C*, endogenous IPs from murine brain lysates were performed from C57B/6 WT mice (4–6 weeks). Endogenous SH2D5 was immunoprecipitated with the anti-SH2D5 antibody, and lysates were immunoblotted for endogenous BCR (*second top panel*). Endogenous BCR was immunoprecipitated with an anti-BCR antibody, and lysates were immunoblotted for endogenous SH2D5 using the anti-SH2D5 antibody (*top panel*). BCR is detected in the SH2D5 immunoprecipitate (*top panel*, *lane 1*), and a faint band corresponding to SH2D5 is present in the BCR immunoprecipitate (*top panel*, *lane 3*, *red asterisk*). Equal expression levels of endogenous BCR and SH2D5 are observed (*two lower panels*, *lanes 1–3*). The IgG heavy chain is indicated as IgG. *D*, to ensure that the SH2D5 antibody was not binding directly to BCR, HEK293T cells were transfected with FLAG-tagged full-length (*FL*) SH2D5 (lane 3) and the truncated mutant (*TM*) lacking the region to which the SH2D5 antibody was raised (*lane 5*; see Fig. 1*C* for schematic). Recombinant SH2D5 was immunoprecipitated with anti-SH2D5 antibodies, and lysates were probed for BCR (*top panel*). *TCL*, total cell lysate. *Asterisk* marks the position of the SH2D5 band in the BCR immunoprecipitate.

tion, it is also abundant in the second extraction with Triton X-100 and sarcosyl, which may be due to the existence of different pools of BCR in the PSD, only some of which coinciding with the SH2D5 pool. In coronal brain sections of C57B/6 WT mice, both proteins share similar expression patterns and are enriched in purkinje cells in the cerebellum (Fig. 5*E*) as well as in pyramidal cells in the cortex. Further enrichment is found for both proteins in the *cornu ammonis* regions of the hippocampus. As a measure of specificity, these signals were absent when the SH2D5 antibody was pre-adsorbed with excess antigen. Taken together, we conclude that both SH2D5 and BCR share similar expressions patterns in brain and show a partial localization within the post-synaptic density.

SH2D5 Depletion in Neurons Reveals a Cell-rounding Phenotype and Reduced Levels of Rac1-GTP—To investigate the function of SH2D5 at the cellular level, we first examined a panel of

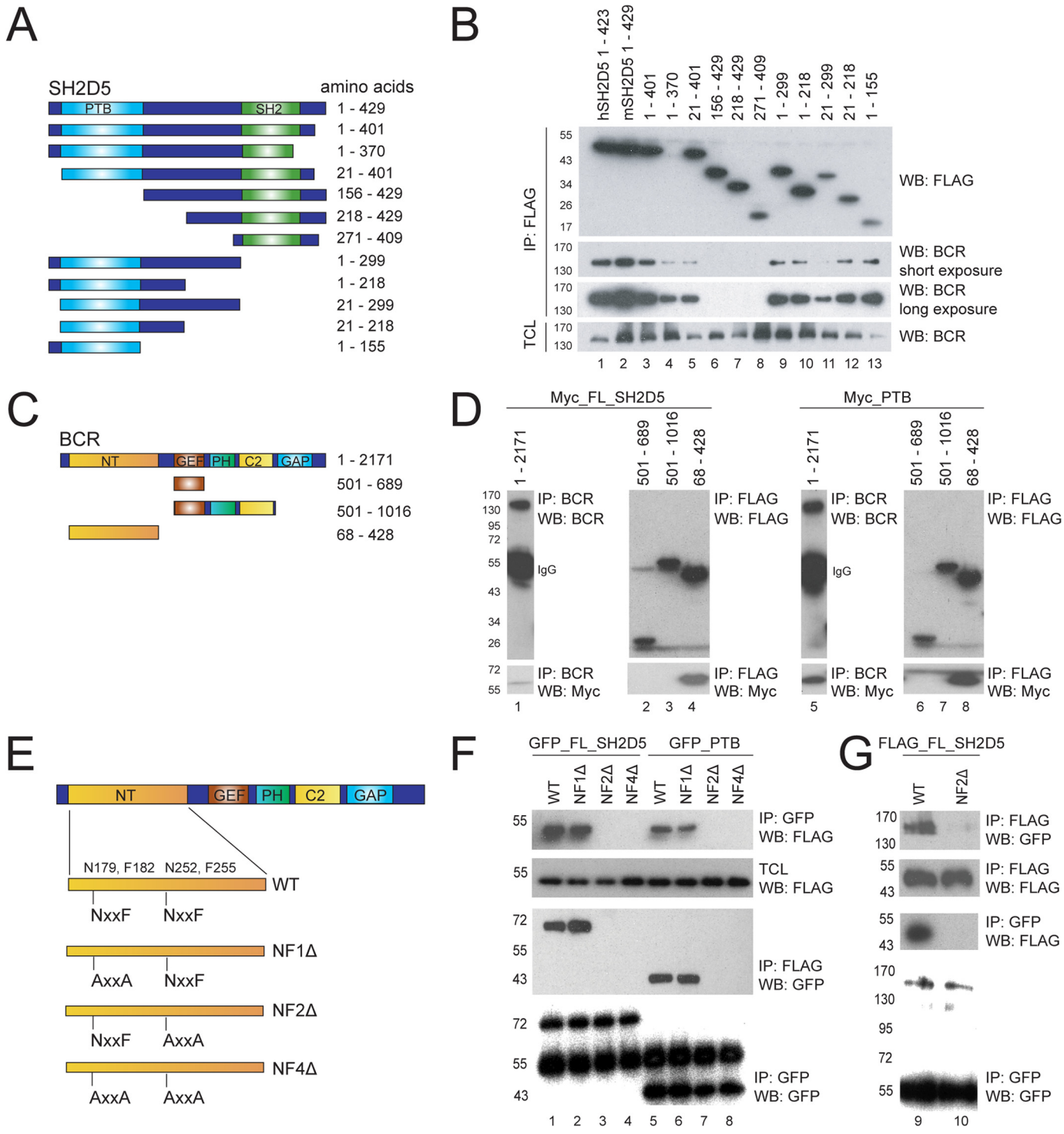

FIGURE 4. **The SH2D5 PTB binds an N*xx*F motif within BCR.** *A*, truncated mutants of mSH2D5 were cloned into an N-terminal 3×FLAG-tagged vector; selected constructs were also cloned into Myc or GFP expression vectors. *B*, FLAG-tagged SH2D5 deletion mutants were transiently transfected into HEK293T cells, and proteins were immunoprecipitated with anti-FLAG antibodies. The presence of endogenous BCR in the immunoprecipitates (*second* and *third panels*) was assayed by BCR immunoblot. Total BCR levels were detected by immunoblotting total cell lysates (*TCL*) of BCR (*bottom panel*). The minimum element required to immunoprecipitate BCR is the SH2D5 PTB domain (*lane 13*). *C*, full-length (*FL*) BCR was cloned into an N-terminal GFP expressing vector and mutants were cloned into an N-terminal 3×FLAG-tagged vector. *D*, FLAG-tagged truncated mutants of BCR and the full-length protein were co-expressed in HEK293T cells along with full-length mSH2D5 and the SH2D5 PTB domain (tagged with a Myc epitope). The N-terminal region of BCR is sufficient to recruit the SH2D5 PTB domain and FL-SH2D5 (*lanes 4* and *8*, *bottom panel*). *E*, BCR mutations, in a FLAG-tagged vector, are defined as follows: N179A, F182A (NF1Δ), N252A, F255A (NF2Δ); and both N*xx*F motifs are defined as follows: N179A, F182A, N252A, and F255A (NF4Δ). *F*, FL-SH2D5 and the SH2D5 PTB domain were immunoprecipitated with GFP antibodies and show equal levels of immunoprecipitation (*bottom panel*). The *middle band* in this panel is the IgG heavy chain. The FL-SH2D5 and the PTB domain are found in the wild-type and NF1Δ BCR immunoprecipitates, as verified by a GFP immunoblot, *lanes 1*, *2*, *5*, and *6*, *second panel* from the *bottom*. Yet, the NF2Δ and NF4Δ fail to immunoprecipitate FL-SH2D5 and the PTB domain, *lanes 3*, *4*, *7*, and *8*, *second panel* from the *bottom*. Neither the FL-SH2D5 nor the PTB domain recruits the NF2Δ and NF4Δ mutant, suggesting that the second N*xx*F motif is required for the SH2D5-BCR interaction. *G*, FL-SH2D5 was cloned into a FLAG vector and the FL-BCR-NF2Δ was generated in a GFP vector. Wild-type FL-BCR immunoprecipitates FL-SH2D5; however, the NF2Δ FL-BCR does not.

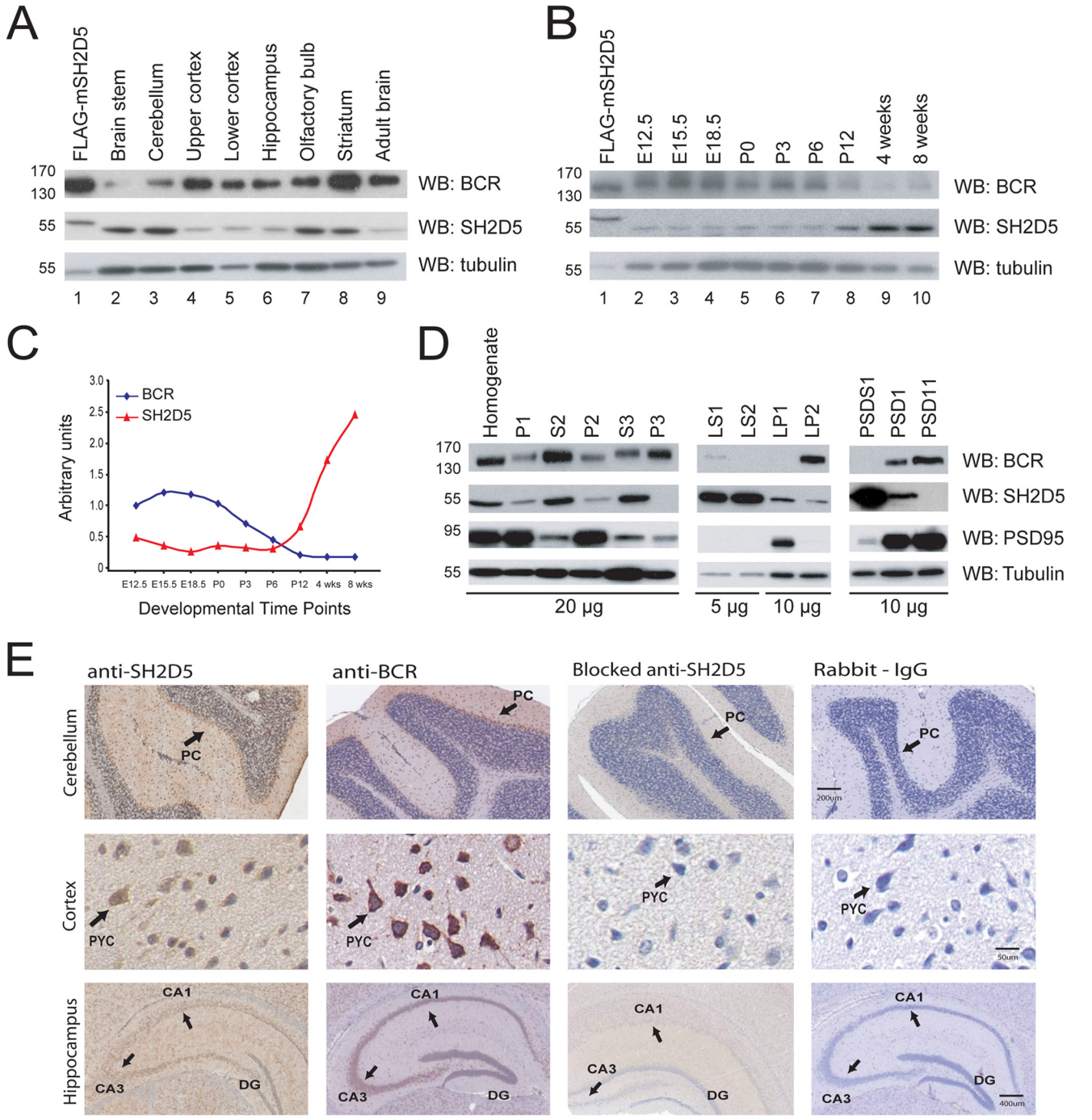

FIGURE 5. **Comparison of BCR and SH2D5 expression patterns in brain.** *A*, lysates were prepared from C57B/6 WT mice aged 4–6 weeks. *B* and *C*, developmental expression of BCR and SH2D5 in brain lysates from embryonic (*E*), postnatal (*P*), and 4- or 8-week-old mice. *Lane 1* in both *A* and *B* is a positive control for the SH2D5 antibody, comprised of overexpressed FLAG-tagged full-length SH2D5 in HEK293T cells. *D*, BCR and SH2D5 expression in postsynaptic density; nuclei/cellular debris (*P1*), supernatant (*S2*), crude synaptosomal fraction (*P2*), cytosol (*S3*), microsomal membranes (*P3*), synaptosomal cytosolic fraction (*LS1*), synaptosol (*LS2*), mitochondria, pre- and postsynaptic membranes (*LP1*), crude synaptic vesicle fraction (*LP2*), PSD fractions extracted with Triton X-100 once and supernatant collected (*PSDSI*), pellet (*PSDI*), and extracted with Triton X-100 and sarcosyl (final concentration, 3%; *PSDII*). *E*, immunohistochemistry on coronal brain sections of cerebellum, cortex, and hippocampus. Both SH2D5 and BCR are enriched in Purkinjie cells (*PC*, *top panel*). The cerebellar nuclear layer has been stained blue with hematoxylin. SH2D5 and BCR expression in pyramidal cells (*PYC*) of the cortex, where BCR is enriched in pyramidal cells compared with SH2D5 (*middle panel*). Finally, SH2D5 and BCR show expression in the *cornu ammonis* (*CA*) regions of the hippocampus (*bottom panel*). No signal is detected upon using rabbit IgG, as a negative control. Likewise, pre-absorption of the anti-SH2D5 antibody, abrogates antibody detection for SH2D5 (blocked anti-SH2D5). *DG*, dentate gyrus. *WB*, Western blot.

cell lines (data not shown) and found endogenous expression of SH2D5 in a B35 neuronal cell line. B35 cells are derived from a rat neuroblastoma and provide a useful model system to ascertain the functional significance of neuronally enriched proteins. Using these cells, we depleted endogenous levels of SH2D5, using the Dharmacon individual siRNAs to SH2D5 in comparison with the Dharmacon SMARTpool and a scrambled control (Fig. 6, *A* and *B*). The siRNA pool resulted in a nearly 50%

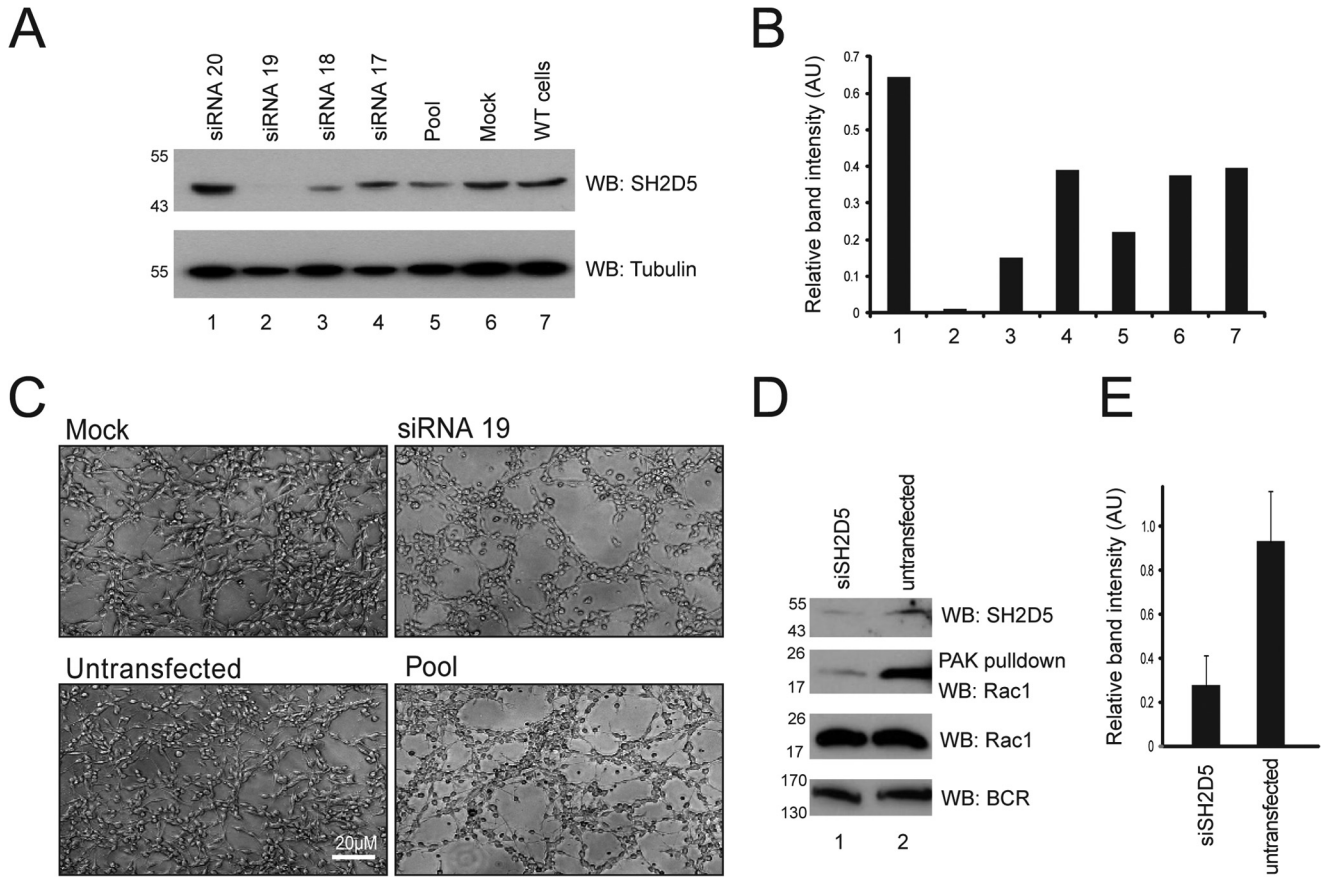

FIGURE 6. **Effect of SH2D5 depletion on the morphology of B35 rat neuroblastoma cells.** *A*, comparison of SH2D5 depletion using 50 nM of nontargeting scrambled and individual SH2D5 siRNAs. The knockdown efficiency of endogenous SH2D5 is ~50% at maximum with the SH2D5 pool. As controls, the individual siRNAs from the Dharmacon SMARTpool (siRNA 17, 18, 19, 20) were compared against the SH2D5 pool along with a mock (no siRNA control) and WT cells. *B*, the individual siRNA no. 19 results in nearly a complete reduction of endogenous SH2D5 (*lane 2*). *C*, images of B35 neurons upon 72 h of siRNA transfection as described in *A*. Cells display a clustered, rounding phenotype, when depleted of SH2D5. Images were taken at 10× magnification. *D*, B35 cells depleted of SH2D5 were assessed for Rac1-GTP levels. Cells were treated with appropriate siRNA and 72 h post-transfection, and GST-PAK assays were performed. As controls, lysates were immunoblotted for levels of total Rac, BCR, and SH2D5. *E*, cells depleted of SH2D5 display reduced levels of Rac1-GTP by ~60%, compared with untreated cells ($n = 2$). The experiment was also repeated using a scrambled siRNA control, which had no effect on activated levels of Rac1, total Rac1, total SH2D5, and total BCR (not shown). *AU*, arbitrary units; *WB*, Western blot.

reduction of endogenous SH2D5, whereas siRNA 19 had a dramatic effect on SH2D5 levels. Upon reducing SH2D5 levels, neurons appeared rounded and grew in a lattice formation. This phenotype was not observed in the scrambled negative controls, in untransfected cells or in the individual siRNAs that did not deplete SH2D5 levels (Fig. 6*C* and data not shown). Attempts to rescue this phenotype with full-length SH2D5 were unsuccessful as cell growth was highly compromised at this stage of the experiment. As low levels of Rac-GTP regulate neuronal cell rounding and BCR has been shown to be a negative regulator of Rac (18, 23), we investigated whether Rac1-GTP levels were affected upon SH2D5 depletion in B35 cells by performing PAK pulldown assays. Indeed, a reduction in endogenous SH2D5 resulted in decreased levels of activated Rac1 (Fig. 6, *D* and *E*).

DISCUSSION

In mediating protein-protein interactions, adaptors bind various types of signaling effectors, including regulators of the actin cytoskeleton such as guanine exchange factor proteins (GEFs) and activating GTPase-activating proteins (GAPs). GEFs and GAPs regulate the activity of small GTPases, wherein GEFs promote the activity of small GTPases and GAPs display an inhibitory effect. In this study, we have characterized an interaction between SH2D5 and BCR, a regulator of Rho GTPases (9, 10) displaying GAP activity toward Rac, Rho, and Cdc42 proteins (18, 23).

The PTB domain of SH2D5 engages with one of two N*xx*F motifs in the N-terminal region of BCR, a binding property demonstrated by other PTB domains. For instance, the Numb PTB domain binds Numb-associated kinase through an N*xx*F motif (24) and to Numb-interacting protein through two tandem N*xx*F motifs on Numb-interacting protein (25). hJIP1 also binds to p190-RhoGEF, through a PTB-N*xx*F interaction (26), which may regulate the cellular localization of p190-RhoGEF in developing neurites.

Our data indicate that the Tyr(P)-independent mode of binding demonstrated by the SH2D5 PTB domain extends to the SH2 domain, as anticipated by the lack of the key βB5 arginine residue required for Tyr(P) recognition by conventional SH2 domains. Yet, while elucidating the binding properties of SH2D5, a tyrosine-phosphorylated protein resolving at 160 kDa was detected in both the wild type and W321R SH2D5 immunoprecipitates, suggesting that SH2D5 could indeed recognize

Tyr(P) ligands. However, BCR is tyrosine-phosphorylated at Tyr-177, which is a docking site for the Grb2 SH2 domain (27). Given that BCR migrates at 160 kDa and would be tyrosine-phosphorylated when intact cells are treated with pervanadate, as was performed in this experiment, we hypothesize that the tyrosine phosphorylated protein identified in the wild type and W321R SH2D5 immunoprecipitates is BCR (and that the interaction does not depend upon the Tyr(P)). Given that cell lines were used in these experiments, we cannot rule out that other *bona fide* Tyr(P) targets of either the SH2D5 PTB or SH2 domain do exist (*e.g.* in PSD).

SH2D5 depletion in neuronal cells was associated with low levels of Rac1-GTP, an observation accompanied by a cell rounding phenotype, which can occur with low levels of activated Rac (28). Neuronal phenotypes associated with altered levels of Rac and Rho include aberrations in cell rounding and adhesion along with neurite outgrowth and retraction (28, 29). Mice deficient for neuronal Rac1 and Rac3 die around postnatal day 13, due to impaired brain development from a reduction of axons and dendrites within the hippocampus. Furthermore, neurogenesis and synaptogenesis within the hippocampus are impaired and axonal projections are reduced in the hippocampus of these mutant mice (30).

In summary, our data support a broader notion that SH2D5 expression in the PSD, its association with BCR and its effect on Rac-GTP may impact synaptic plasticity, which is important for learning and memory.

Acknowledgments—We thank N. Heisterkamp for providing the kind gift of the GFP-BCR construct. We also thank Wade Dunham for critical review of the manuscript.

REFERENCES

1. Schlessinger, J., and Lemmon, M. A. (2003) SH2 and PTB domains in tyrosine kinase signaling. *Sci. STKE* 2003, RE12
2. Uhlik, M. T., Temple, B., Bencharit, S., Kimple, A. J., Siderovski, D. P., and Johnson, G. L. (2005) Structural and evolutionary division of phosphotyrosine binding (PTB) domains. *J. Mol. Biol.* **345,** 1–20
3. Pawson, T. (2007) Dynamic control of signaling by modular adaptor proteins. *Curr. Opin. Cell Biol.* **19,** 112–116
4. Liu, B. A., and Nash, P. D. (2012) Evolution of SH2 domains and phosphotyrosine signalling networks. *Philos. Trans. R. Soc. Lond B. Biol. Sci.* **367,** 2556–2573
5. Pawson, T., Gish, G. D., and Nash, P. (2001) SH2 domains, interaction modules and cellular wiring. *Trends Cell Biol.* **11,** 504–511
6. Lein, E. S., Hawrylycz, M. J., Ao, N., Ayres, M., Bensinger, A., Bernard, A., Boe, A. F., Boguski, M. S., Brockway, K. S., Byrnes, E. J., Chen, L., Chen, L., Chen, T. M., Chin, M. C., Chong, J., Crook, B. E., Czaplinska, A., Dang, C. N., Datta, S., Dee, N. R., Desaki, A. L., Desta, T., Diep, E., Dolbeare, T. A., Donelan, M. J., Dong, H. W., Dougherty, J. G., Duncan, B. J., Ebbert, A. J., Eichele, G., Estin, L. K., Faber, C., Facer, B. A., Fields, R., Fischer, S. R., Fliss, T. P., Frensley, C., Gates, S. N., Glattfelder, K. J., Halverson, K. R., Hart, M. R., Hohmann, J. G., Howell, M. P., Jeung, D. P., Johnson, R. A., Karr, P. T., Kawal, R., Kidney, J. M., Knapik, R. H., Kuan, C. L., Lake, J. H., Laramee, A. R., Larsen, K. D., Lau, C., Lemon, T. A., Liang, A. J., Liu, Y., Luong, L. T., Michaels, J., Morgan, J. J., Morgan, R. J., Mortrud, M. T., Mosqueda, N. F., Ng, L. L., Ng, R., Orta, G. J., Overly, C. C., Pak, T. H., Parry, S. E., Pathak, S. D., Pearson, O. C., Puchalski, R. B., Riley, Z. L., Rockett, H. R., Rowland, S. A., Royall, J. J., Ruiz, M. J., Sarno, N. R., Schaffnit, K., Shapovalova, N. V., Sivisay, T., Slaughterbeck, C. R., Smith, S. C., Smith, K. A., Smith, B. I., Sodt, A. J., Stewart, N. N., Stumpf, K. R., Sunkin, S. M., Sutram, M., Tam, A., Teemer, C. D., Thaller, C., Thompson, C. L., Varnam, L. R., Visel, A., Whitlock, R. M., Wohnoutka, P. E., Wolkey, C. K., Wong, V. Y., Wood, M., Yaylaoglu, M. B., Young, R. C., Youngstrom, B. L., Yuan, X. F., Zhang, B., Zwingman, T. A., and Jones, A. R. (2007) Genome-wide atlas of gene expression in the adult mouse brain. *Nature* **445,** 168–176
7. Trinidad, J. C., Specht, C. G., Thalhammer, A., Schoepfer, R., and Burlingame, A. L. (2006) Comprehensive identification of phosphorylation sites in postsynaptic density preparations. *Mol. Cell Proteomics* **5,** 914–922
8. Munton, R. P., Tweedie-Cullen, R., Livingstone-Zatchej, M., Weinandy, F., Waidelich, M., Longo, D., Gehrig, P., Potthast, F., Rutishauser, D., Gerrits, B., Panse, C., Schlapbach, R., and Mansuy, I. M. (2007) Qualitative and quantitative analyses of protein phosphorylation in naive and stimulated mouse synaptosomal preparations. *Mol. Cell Proteomics* **6,** 283–293
9. Oh, D., Han, S., Seo, J., Lee, J. R., Choi, J., Groffen, J., Kim, K., Cho, Y. S., Choi, H. S., Shin, H., Woo, J., Won, H., Park, S. K., Kim, S. Y., Jo, J., Whitcomb, D. J., Cho, K., Kim, H., Bae, Y. C., Heisterkamp, N., Choi, S. Y., and Kim, E. (2010) Regulation of synaptic Rac1 activity, long-term potentiation maintenance, and learning and memory by BCR and ABR Rac GTPase-activating proteins. *J. Neurosci.* **30,** 14134–14144
10. Um, K., Niu, S., Duman, J. G., Cheng, J. X., Tu, Y. K., Schwechter, B., Liu, F., Hiles, L., Narayanan, A. S., Ash, R. T., Mulherkar, S., Alpadi, K., Smirnakis, S. M., and Tolias, K. F. (2014) Dynamic control of excitatory synapse development by a Rac1 GEF/GAP regulatory complex. *Dev. Cell* **29,** 701–715
11. Colwill, K., Wells, C. D., Elder, K., Goudreault, M., Hersi, K., Kulkarni, S., Hardy, W. R., Pawson, T., and Morin, G. B. (2006) Modification of the Creator recombination system for proteomics applications–improved expression by addition of splice sites. *BMC Biotechnol.* **6,** 13
12. Letunic, I., Doerks, T., and Bork, P. (2009) SMART 6: recent updates and new developments. *Nucleic Acids Res.* **37,** D229–D232
13. Dunah, A. W., Hueske, E., Wyszynski, M., Hoogenraad, C. C., Jaworski, J., Pak, D. T., Simonetta, A., Liu, G., and Sheng, M. (2005) LAR receptor protein tyrosine phosphatases in the development and maintenance of excitatory synapses. *Nat. Neurosci.* **8,** 458–467
14. Kessner, D., Chambers, M., Burke, R., Agus, D., and Mallick, P. (2008) ProteoWizard: open source software for rapid proteomics tools development. *Bioinformatics* **24,** 2534–2536
15. Deutsch, E. W., Mendoza, L., Shteynberg, D., Farrah, T., Lam, H., Tasman, N., Sun, Z., Nilsson, E., Pratt, B., Prazen, B., Eng, J. K., Martin, D. B., Nesvizhskii, A. I., and Aebersold, R. (2010) A guided tour of the TransProteomic Pipeline. *Proteomics* **10,** 1150–1159
16. Liu, G., Zhang, J., Larsen, B., Stark, C., Breitkreutz, A., Lin, Z. Y., Breitkreutz, B. J., Ding, Y., Colwill, K., Pasculescu, A., Pawson, T., Wrana, J. L., Nesvizhskii, A. I., Raught, B., Tyers, M., and Gingras, A. C. (2010) ProHits: integrated software for mass spectrometry-based interaction proteomics. *Nat. Biotechnol.* **28,** 1015–1017
17. Chen, G. I., and Gingras, A. C. (2007) Affinity-purification mass spectrometry (AP-MS) of serine/threonine phosphatases. *Methods* **42,** 298–305
18. Cho, Y. J., Cunnick, J. M., Yi, S. J., Kaartinen, V., Groffen, J., and Heisterkamp, N. (2007) Abr and Bcr, two homologous Rac GTPase-activating proteins, control multiple cellular functions of murine macrophages. *Mol. Cell. Biol.* **27,** 899–911
19. Kaartinen, V., Gonzalez-Gomez, I., Voncken, J. W., Haataja, L., Faure, E., Nagy, A., Groffen, J., and Heisterkamp, N. (2001) Abnormal function of astroglia lacking Abr and Bcr RacGAPs. *Development* **128,** 4217–4227
20. Tan, E. C., Leung, T., Manser, E., and Lim, L. (1993) The human active breakpoint cluster region-related gene encodes a brain protein with homology to guanine nucleotide exchange proteins and GTPase-activating proteins. *J. Biol. Chem.* **268,** 27291–27298
21. Forman-Kay, J. D., and Pawson, T. (1999) Diversity in protein recognition by PTB domains. *Curr. Opin. Struct. Biol.* **9,** 690–695
22. Li, S. C., Zwahlen, C., Vincent, S. J., McGlade, C. J., Kay, L. E., Pawson, T., and Forman-Kay, J. D. (1998) Structure of a Numb PTB domain-peptide complex suggests a basis for diverse binding specificity. *Nat. Struct. Biol.* **5,** 1075–1083
23. Chuang, T. H., Xu, X., Kaartinen, V., Heisterkamp, N., Groffen, J., and Bokoch, G. M. (1995) Abr and Bcr are multifunctional regulators of the Rho GTP-binding protein family. *Proc. Natl. Acad. Sci. U.S.A.* **92,**

10282–10286
24. Chien, C. T., Wang, S., Rothenberg, M., Jan, L. Y., and Jan, Y. N. (1998) Numb-associated kinase interacts with the phosphotyrosine binding domain of Numb and antagonizes the function of Numb *in vivo*. *Mol. Cell. Biol.* **18,** 598–607
25. Qin, H., Percival-Smith, A., Li, C., Jia, C. Y., Gloor, G., and Li, S. S. (2004) A novel transmembrane protein recruits numb to the plasma membrane during asymmetric cell division. *J. Biol. Chem.* **279,** 11304–11312
26. Meyer, D., Liu, A., and Margolis, B. (1999) Interaction of c-Jun amino-terminal kinase interacting protein-1 with p190 rhoGEF and its localization in differentiated neurons. *J. Biol. Chem.* **274,** 35113–35118
27. Ma, G., Lu, D., Wu, Y., Liu, J., and Arlinghaus, R. B. (1997) Bcr phosphorylated on tyrosine 177 binds Grb2. *Oncogene* **14,** 2367–2372
28. Caron, E. (2003) Rac signalling: a radical view. *Nat. Cell Biol.* **5,** 185–187
29. Etienne-Manneville, S., and Hall, A. (2002) Rho GTPases in cell biology. *Nature* **420,** 629–635
30. Corbetta, S., Gualdoni, S., Ciceri, G., Monari, M., Zuccaro, E., Tybulewicz, V. L., and de Curtis, I. (2009) Essential role of Rac1 and Rac3 GTPases in neuronal development. *FASEB J.* **23,** 1347–1357